The transmembrane leucine-rich repeat protein DMA-1 promotes dendrite branching and growth in *C. elegans*

Oliver W. Liu and **Kang Shen**

Howard Hughes Medical Institute, Department of Biology, Stanford University, 385 Serra Mall, Stanford, CA 94305, kangshen@stanford.edu

Abstract

Dendrites often adopt complex branched structures. The development and organization of these arbors fundamentally determine the potential input and connectivity of a given neuron. The cell-surface receptors that control dendritic branching remain poorly understood. Here, we show that in *Caenorhabditis elegans*, a previously uncharacterized transmembrane protein containing extracellular leucine-rich repeat (LRR) domains, which we name DMA-1 (*D*endrite-*M*orphogenesis-*A*bnormal), promotes dendrite branching and growth. Sustained expression of *dma-1* is found only in the elaborately branched sensory neurons PVD and FLP. Genetic analysis showed that loss of *dma-1* causes much reduced dendritic arbors while overexpression of *dma-1* results in excessive branching. Forced expression of *dma-1* in neurons with simple dendrites was sufficient to promote ectopic branching. Animals lacking *dma-1* are defective in sensing harsh touch. DMA-1 is the first transmembrane LRR protein to be implicated in dendritic branching and expands the breadth of roles played by LRR receptors in nervous system development.

Dendritic arbors adopt diverse branched morphologies of varying complexity that are characteristic for a given neuron type [1,2]. The organization of the dendritic arbors is fundamental to the connectivity and function of a neuron, determining both the potential receptive field and the sampling and processing of signals within that field [3]. For example, in the mammalian retina, there are about 12 types of retinal ganglion cells (RGCs) and 30 types of amacrine cells [1]. Each RGC and amacrine cell type exhibits a characteristic combination of dendritic field size, branch complexity, and dendritic targeting area. An essential step in the development of these complex dendrite morphologies is the regulation of dendrite branching.

While fundamental to the shape and connectivity of the nervous system, the mechanisms that regulate dendrite branching are not well understood, though a variety of pathways have been implicated in the process. In mammals, reduced activity of the transcriptional factors NeuroD and Crest, which are widely expressed in the nervous system, results in decreased dendritic branching and growth in certain cell types [4,5]. Secreted ligands, like Semaphorin 3A, can promote dendritic branching and spine maturation in mouse cortical neurons [6].

The majority of our understanding of the molecular mechanisms involved in dendritic branching comes from studies of the dendritic arborization neurons found in *Drosophila melanogaster*. The study of the four classes of dendritic arborization neurons, which vary by complexity of branching, has helped illuminate important dendrite organizational principles

such as the ability to identify and avoid sister dendrites from the same neuron (self-avoidance), and the ability of dendrites from neurons of the same cell-type to minimally overlap (tiling) [7,8]. Genetic screens utilizing dendritic arborization neurons have identified intracellular pathways that regulate levels of branching, including mechanisms involving transcriptional regulation [9,10], actin and microtubule-dependent trafficking [11,12], secretion/endocytosis [13,14], signal transduction [15,16], and RNA localization [17]. These pathways function, in large part, to mobilize the cellular machinery needed for dendrite growth [8]. Conspicuously absent from our molecular understanding of dendrite branching has been the identity of cell surface proteins promoting this process. Organized dendrite branching must ultimately be defined and instructed by extracellular interactions, yet the cell-surface receptors involved in activating dendritic branching pathways remain, for the most part, unknown.

In the model nematode *Caenorhabditis elegans,* where most neurons are morphologically simple, two sets of sensory neurons, PVD in the body and FLP in the head, adopt complex, highly branched and highly organized dendrite structures with features that resemble the "self-avoidance" and "tiling" principles seen in dendritic arborization neurons [18,19]. The genetic and experimental tractability of *C. elegans* make the PVD and FLP neurons attractive, novel systems in which to study mechanisms that regulate dendrite branching.

The immense complexity of nervous system development is made possible by a multitude of receptor-ligand interactions on the surfaces of neurons [20,21]. Transmembrane LRR (leucine-rich repeat) proteins often are expressed exclusively in the nervous system, and extracellular LRR domains can serve as protein-protein interaction motifs, suggesting that they participate in important receptor-ligand interactions [22,23]. Indeed, specific roles for transmembrane LRR proteins have recently been uncovered in synaptogenesis and dendrite targeting [24-27]. Still, the functions of most neuronally expressed transmembrane LRR proteins remain unknown. Here, in order to identify potential functions of transmembrane LRR proteins in the *C. elegans* nervous sytem, we initiated an effort to determine the expression and localization pattern of every type-1 transmembrane LRR protein in the *C. elegans* genome. Through this analysis, we identified a gene we call *dma-1* (*T10G9.3; d*endrite *m*orphogenesis *a*bnormal-1), which demonstrated sustained expression in only two sets of neurons, PVD and FLP, suggesting a model where this cell-surface receptor acts as an intrinsic factor to promote dendrite branching and growth. We provide additional evidence supporting this model, which expands the breadth of known functions played by LRR proteins in nervous system development, and demonstrates the importance of cell-surface interactions in controlling dendrite branching.

Results

Neuronally expressed transmembrane LRR proteins

In *C. elegans*, 17 genes are predicted to encode type-1 transmembrane proteins with extracellular LRR domains [22]. In order to determine the expression and localization patterns of these LRR proteins, we systematically generated tagged transgenes utilizing a precise fosmid recombineering technique which preserves upstream, downstream, and intronic genome sequences [28] (Fig. S1). This approach allowed us to accurately determine the *in vivo*

expression of these proteins since we maintained all likely regulatory sequences in the tagged transgene. Using this strategy, we identified six transmembrane LRR proteins that are expressed predominantly in the nervous system (Table S1).

When examining these expression patterns, we noted that the previously uncharacterized gene *T01G9.3*, which we have named *dma-1*, is expressed in a unique subset of neurons. *dma-1* is predicted to encode a 603 aa transmembrane protein with an extracellular region composed of 15 LRR motifs and a short intracellular region (73 aa) with no obvious domains (Fig. 1a). Sustained expression of DMA-1 is found most prominently in two pairs of sensory neurons, PVD and FLP (Fig. 1b–c). Notably, these neurons are by far the most highly branched neurons in *C. elegans*, extending elaborate dendrite arbors that envelop the body and head respectively [18,19,29]. The remaining 298 neurons in *C. elegans* contain few or no branches. Expression of DMA-1 can be detected in PVD neurons immediately after the cells are born during the L2 larval stage, but before extensive branching of these neurons has initiated (Fig. S2a). DMA-1 can also be detected transiently in other head neurons (including the SIA, SIB, SMB and/or SMD classes of neurons based on the presence of processes along the sub-lateral cords), ventral cord neurons, and the vulva during larval and early adult stages (Fig. S2b–d) This provocative expression pattern of DMA-1 in primarily PVD and FLP prompted us to investigate potential roles for *dma-1* in dendrite branching and morphogenesis.

dma-1 mutants are defective in dendrite morphogenesis

We examined PVD morphology using a cell specific marker (*ser2prom3∷myrGFP*) that clearly labels the entire neuron (Fig. 2a). PVD neurons (PVDR and PVDL) are generated post-embryonically in the lateral posterior body during the L2 larval stage. Only recently has the extent of dendritic branching in PVD been appreciated [18,19,29,30]. The neurons send out three primary (1°) processes: anteriorly- and posteriorly-directed dendritic processes, which run laterally along the worm body, and a ventrally-directed axon, which enters the ventral nerve cord as a commissure and then migrates anteriorly along the nerve cord. During the subsequent larval stages (late L2 – L4), a series of orthogonal secondary (2°), tertiary (3°), and quaternary (4°) level branches emerges resulting in an array of branched structural units resembling candelabras which decorate the initial 1° dendritic processes (Figs. 2b and S3a). 2° processes can branch prior to reaching the 3° level, creating secondary prime (2°′) branches. Multiple organizing principles seen in other models of dendritic branching, such as *Drosophila melanogaster* dendritic arborization neurons, are evident in the development of PVD, including regions of restricted branching, self-avoidance between sister dendrites, and rough tiling between PVD and FLP branches [19]. In PVD, the frequency of 2°′ branching between the 1° and 3° levels is low, and adjacent 3° processes do not overlap even as they grow towards each other (Fig. 2b). To determine the role of *dma-1* in PVD dendrite development, we generated a null allele, *wy686*, by deleting a region of the genome from ~3kb upstream of the *dma-1* start site to the 3′ end of the gene using the recently developed *Mos*Del technique [31]. When we crossed the PVD marker into the *dma-1(wy686)* mutant background strain and examined L4 animals, we observed a fully penetrant dendrite branching phenotype (Fig. 2c). While the anterior 1° dendritic process showed normal outgrowth in the majority of animals (the remaining animals displayed some reduction in

dendrite length, Fig. S3b), candelabra structures never developed along the 1° branch. 2° branches grew minimally and often branched and/or appeared to be fused with adjacent 2° branches before reaching the 3° level. 3° and 4° branches were largely absent. The posterior 1° dendritic process exhibited similar loss of candelabra formation and highly penetrant growth defects (Fig. S3c). Interestingly, the ventral axon appeared morphologically normal, suggesting that *dma-1* is specifically required for development of dendrites. *dma-1* knockdown by feeding RNAi caused similar dendrite branching phenotypes in ∼50% of animals (Fig. S4).

The qualitative defect in dendrite morphologies we observed in *dma-1 (wy686)* mutants could be due to decreases in the amount of 2° branching and/or aberrant outgrowth of these 2° branches. In order to quantitatively measure these effects, we chose to study mid-L3 larval stage worms. By mid-L3, in wildtype PVD neurons, stable 2° branches have developed and are in the process of 3° and 4° branch elaboration (Fig. S2a). As a result, this time point offers high resolution for observing defects in 2° branch formation and outgrowth, allowing us to easily measure both the frequency and length of 2° branches (Fig. 2d–e). We found that in *dma-1(wy686)*, the frequency of 2° branches decreased 44% compared to wild type. Furthermore, the average length of 2° branches decreased by 47% (Fig. 2f–g). Thus, the abnormal dendrite morphology in *dma-1(wy686)* is due to a combination of decreased levels of 2° branching as well as decreased outgrowth of these 2° processes, which results in complete loss of higher order branches.

DMA-1 cell autonomously regulates dendrite morphogenesis

The expression analysis described above demonstrated that *dma-1* is strongly expressed in PVD and not in neighboring neurons or tissue, suggesting that DMA-1 functions cell autonomously in PVD to promote branching. Consistent with this model, we could rescue the PVD morphology defects in *dma-1(wy686)* by expressing *dma-1* cDNA from a PVD-specific promoter (Fig. 3a–b). We generated two lines in which ∼80% of animals demonstrated at least partial rescue (Fig. 3c). In fully rescued animals (56% and 61%), dendrite outgrowth, dendrite branching, and formation of candelabra structures were indistinguishable from wild-type, demonstrating that *dma-1* acts cell autonomously in PVD neurons to promote dendrite branching and growth.

To determine the subcellular localization of *dma-1* within PVD, we expressed a GFP-tagged *dma-1* transgene using a PVD-specific promoter (Fig. 3d). We found all dendritic processes to be labeled with this tagged protein and single slice imaging of the cell body confirmed that DMA-1: :GFP can be found on the cell surface (Fig. S5). We also observed numerous bright puncta in the cell body and dendritic processes. Notably, the PVD axon was not well labeled by DMA-1: :GFP, indicating that DMA-1 is a dendrite-specific protein, consistent with DMA-1 playing a direct role in regulating dendrite morphogenesis. Similar to PVD, the FLP neurons are highly branched (Fig. 4a) and express *dma-1* (Fig. 1c). We found that FLP branching is severely compromised in the *dma-1(wy686)* mutants (Fig. 4b) and that this phenotype can be rescued by FLP-specific expression of *dma-1* (Figs. 4c and S6). Thus *dma-1* functions cell autonomously in both sets of highly branched neurons in worms to promote arborization.

DMA-1 overexpression causes excessive dendrite branching

To determine whether the activity of DMA-1 is rate-limiting for dendritic branching, we examined the effects of *dma-1* overexpression in wild-type animals. We found that *dma-1* overexpression resulted in excessive branching of PVD (Fig. 5a–b). Instead of the well-arrayed candelabra structures found in wild-type, animals carrying the *dma-1* overexpression array developed tangled networks of dendritic branches. While the general organization of 1°, 2°, 3°, and 4° level branches could be distinguished, uncontrolled dendrite branching and growth were evident. The frequency of 2° branching along the 1° processes increased by 58%. The amount of 2°′ branching in the regions between the 1° and 3° processes increased ~7 fold (Fig. 5c–d). The majority of these 2° and 2°′ processes did not grow orthogonally to the 1° processes indicating that these branches were not properly guided to the 3° branch level. Finally, the characteristic self-avoidance of sister dendrites seen in wildtype worms was lost in worms overexpressing *dma-1*. 2° and 2°′ processes often intersected and/or fused, while almost all 3° processes overlapped with adjacent 3° processes (Fig. 5b). To quantify this loss of self-avoidance, we calculated an Avoidance Index (AI) by comparing the number of visible gaps between 3° branches to the number of candelabra in a given worm (Fig. 5e). In wild-type worms, this ratio is ~1 (1.00 +/− 0.02 s.e.m.) since there is a gap between each candelabra. As 3° branches overlap, the AI decreases. In worms overexpressing *dma-1*, we observed a dramatic reduction in the AI (0.20 +/− 0.04 s.e.m.) demonstrating a severe defect in 3° self-avoidance.

Expression of a truncated version of DMA-1 that lacks the transmembrane and cytoplasmic domains (*dma-1 tm)* from a PVD-specific promoter did not rescue PVD morphology defects in *dma-1(wy686)* animals or result in overbranching in wild-type worms, indicating that the transmembrane domain of DMA-1 is required for its function in PVD branching (data not shown).

Ectopic expression of DMA-1 induces branching

Consistent with our conclusions from the loss-of-function experiments, the overexpression phenotypes demonstrate a role for *dma-1* in activation of pathways involved in dendrite branching and growth. To further test this hypothesis, we asked if expression of *dma-1* was sufficient to induce branching in neurons that normally do not branch extensively. We chose two sets of sensory neurons, PDE and PLM, which 1) display simple architectures with a single branch point, thus demonstrating that they have the potential to branch, 2) do not express detectable levels of *dma-1*, and 3) send out processes that are closely positioned to PVD processes so that the extracellular environment is likely to be conducive to DMA-1 receptor activation (Fig. 6a, b, e). In both cases, we found that cell-specific expression of *dma-1* results in ectopic branching of these neurons in 25-30% of animals (Fig. 6d, g). Interestingly, in PDE, orthogonal ectopic branches appeared at a stereotyped position in the commissure of PDE, corresponding to the region where 3° level branches emerge in PVD (Fig. 6c), suggesting that an activating ligand is localized to discrete locations in the worm. In PLM, ectopic branches are seen along the sublateral process, which runs parallel to 3° processes of PVD (Fig. 6f). Thus, in morphologically simple neurons neighboring PVD, ectopic expression of *dma-1* is sufficient to activate branching pathways in certain extracellular environments. Expression of *dma-1 tm* in PDE or PLM did not result in

ectopic branching (multiple transgenic lines tested), indicating that ectopic branching observed in PDE and PLM requires functional DMA-1 and is not due simply to overexpression of a non-specific LRR protein (Fig. 6d, g). Ectopic expression of full length *dma-1* in OLL head neurons did not result in increased dendritic complexity in these neurons, supporting the hypothesis that activation of DMA-1 is context-dependent within the animal (data not shown).

Loss of *dma-1* causes defects in harsh touch response

PVD has been shown to play a role in responding to multiple stimuli including strong mechanical stimulation (harsh touch) [32,33]. The similarity in form and function between PVD and multi-dendritic nociceptors from other organisms suggests that the highly branched dendritic morphology of PVD plays an important role in its ability to sense stimuli. As *dma-1* mutant animals demonstrate greatly reduced PVD branching, we tested if loss of *dma-1* also results in a defect in PVD sensory function.

Animals respond to prodding in the midsection of the body (vulva harsh touch) by initiating forwards or backwards locomotion. This behavior is dependent on PVD and the touch receptor neurons (ALM, AVM, PLM, PVM). PVD function is typically assessed in a *mec-4* mutant background, which lacks functioning touch receptor neurons. As controls, we found that *mec-4(u253)* and *dma-1(wy686)* single mutant animals demonstrate wild-type responses to harsh touch (∼90% of worms initiate backing), while only 20% of *mec-3(e1338)* mutant animals, which lack function in both PVD and the touch receptor neurons, respond to harsh touch (Fig. 7). Additional neurons involved in sensing harsh touch likely account for the remaining response measured in *mec-3(e1338)* animals [33]. We found that *dma-1(wy686) mec-4(u253)* double mutant animals display an intermediate defect in response to harsh touch (∼64% of worms initiate backing). Expression of *dma-1* from a PVD-specific promoter in *dma-1(wy686) mec-4(u253)* double mutant animals partially rescues the sensory defect in these animals indicating that DMA-1 functions cell autonomously in PVD to affect the response to harsh touch and is consistent with the hypothesis that the dendrite morphology of PVD is critical in determining the sensory input to the neuron and thus its function (Fig. 7). The lack of complete rescue of the harsh touch response defect in these animals is consistent with partial rescue of the PVD morphology defect in animals expressing PVD-specific DMA-1.

Discussion

Using a systematic fosmid-tagging approach to simultaneously characterize expression and sub-cellular localization patterns, we endeavored to identify the genomic complement of cell-surface LRR receptor proteins important in the development and function of the nervous system. Our goals for this approach were to not only simply determine which transmembrane LRR proteins are expressed in the nervous system, but to also use the precise identity of the neurons in these expression patterns to deduce aspects of the protein function. Here, with DMA-1, we present an instance where, indeed, the unique expression pattern of the protein provided remarkable insight into its role in regulating dendrite branching.

A pattern of sustained expression in primarily PVD and FLP has not been previously reported for any other gene in *C. elegans* (http://genome.sfu.ca/gexplore/) [34]. Genes involved in mechanosensation, such as *mec-3* and *mec-10*, are expressed in PVD and FLP, but also in the six touch receptor neurons (ALML, ALMR, PLML, PLMR, AVM, PVM), suggesting that DMA-1 is not involved in mechanosensation in general. Instead, this pattern intimates a role for DMA-1 in the property unique to PVD and FLP in the *C. elegans* nervous system: highly branched dendrites. Our genetic characterization of *dma-1* supports a model where DMA-1 functions as an intrinsic factor on the cell-surface of dendrites which can activate dendrite branching and growth pathways. Loss-of-function mutants suffer severe reductions in PVD and FLP dendrite branching and growth. These defects are rescued in the mutant by PVD or FLP cell-specific expression of *dma-1*, demonstrating DMA-1 acts cell autonomously to regulate this phenotype. Strikingly, overexpression of *dma-1* was sufficient to generate a highly overbranched PVD morphology, indicating that the level of DMA-1 is rate-limiting for generating dendritic branches. This property is similar to what has been observed in *D. melanogaster* dendritic arborization neurons where expression levels of the transcription factor CUT determine the degree of dendritic branching. Similarly, with DMA-1, we have identified a factor intrinsic to PVD whose expression level determines the level of PVD dendritic branching. Instead of a transcription factor, however, we have identified a cell surface receptor, suggesting that in PVD, one rate-limiting control of dendrite branching is the processing of external cues by surface receptors.

Dendritic morphology is regulated both by growth promoting and growth inhibiting factors. In *D. melanogaster*, self avoidance is elegantly mediated by the strict homotypic binding properties of different splice variants of the cell adhesion molecule DSCAM [35]. Recent time lapse imaging of PVD 3° branches in *C. elegans* suggest that self-avoidance in PVD is also initiated by branch-branch contact [19]. Upon *dma-1* overexpression, we observed a loss of self avoidance between the PVD 3° branches in addition to overbranching, indicating that in these animals, the mechanisms to regulate self-avoidance are diminished and/or are no longer sufficient. As DMA-1 promotes dendritic growth, as well as branching, it is possible the growth promoting signals provided by overexpressed DMA-1 overpowers contact dependent mechanisms that control 3° length.

The specific expression pattern of DMA-1 prompted us to ask whether DMA-1 is sufficient to generate dendritic branches. We observed ectopic branches in PDE and PLM when we ectopically expressed DMA-1 in these morphologically simple neurons, providing additional evidence that DMA-1 is sufficient to at least partially activate dendrite branching pathways. Of note, the degree of ectopic branching on PDE and PLM is clearly lower than the amount of branching usually seen in PVD and FLP, indicating that we have not fully recapitulated the molecular pathways involved in DMA-1 mediated branching. It is possible that, although PDE and PLM processes are often in close proximity to PVD processes, they still do not receive all the appropriate external cues/binding partners that activate DMA-1 in PVD. It is also possible that PDE and PLM do not have sufficient levels of intracellular factors, such as high levels and distal localization of golgi and endosomes, necessary for building a highly branched structure. Intriguingly, ectopic branches in PDE were found at a highly stereotyped location on the PDE commissure, suggesting that the activating partner of DMA-1 is

spatially regulated and that DMA-1 is involved in local cell-cell interactions that activate branching. This would make DMA-1 the first contact dependent receptor known to promote dendritic branching. The stereotyped nature of dendritic structures in general has long been appreciated, suggesting a requirement for close interaction between a neuron and its surrounding tissue for proper spatial regulation of dendrite branching [1,2]. Yet, the surface proteins involved in cell-cell interactions that activate dendritic branching are not well established. Diffusible factors, such as Slit or semaphorins, nerve growth factor (NGF), and brain-derived neurotrophic factor (BDNF) have been shown to influence aspects of dendrite morphology, but these are not dependent on cell-cell contact [6,36,37]. The immunoglobulin superfamily protein Turtle has been suggested to restrict dendrite branching in low complexity dendritic arborization neurons in *Drosophila* [38]. The identification of proteins that interact with DMA-1 will be an important step in determining the extracellular mechanism of DMA-1 activation.

Besides PVD and FLP, expression of DMA-1 can also be transiently detected in other head neurons and ventral cord motor neurons. These neurons do not display extensive branching, suggesting that they perhaps utilize DMA-1 primarily to regulate growth of processes. Interestingly, besides FLP, the head neurons that display the most consistent expression of DMA-1 elaborate processes that grow along the dorsal and ventral sub-lateral cords, which are the same boundaries along which the tertiary branches of PVD grow. These data suggest that DMA-1 may play a role in regulating growth and branching along the sub-lateral boundaries and support the model that the activating ligand of DMA-1 may be localized in these regions.

Based on sequence alone, the identity of a DMA-1 binding partner is difficult to predict. The leucine-rich repeat structural motif forms a curved solenoid structure that provides a surface suited for many types of protein-protein interactions [39]. For example, LRR domains have been shown to interact with the Ig domains in Robo [40], the LNS domains of neurexin [24], and the N-terminal domain of human E-cadherin [41]. While the variety of potential interactors may make identification of LRR binding partners more difficult, it is precisely this combination of breadth and specificity that makes LRR transmembrane proteins particularly intriguing candidates to be mediators of the complexity of nervous system development and function. DMA-1 is the first transmembrane LRR protein shown to function in nervous system development in *C. elegans* and is the first transmembrane LRR protein implicated in dendritic branching. A close homolog to DMA-1 exists in flies (*reduced ocelli*) which is expressed throughout the nervous system [42], suggesting that interactions involving this class of extracellular LRR transmembrane proteins will be conserved in nervous system development of other species.

Methods

Strains and genetics

Worms were rasied on OP50 *Escherichia coli*-seeded nematode growth medium (NGM) plates at 20°C. N2 Bristol was used as the wild-type reference strain. Strain IE22994 containing the ttTi22997 transposon insertion upstream of *dma-1* was obtained from L. Segalat. CX6365 *rrf-1(pk1426)* was obtained from C. Kenyon. TV8378 *pha-1(e2123ts)* was

obtained from A. Fire. TU253 *mec-4(u253)* and CB1338 *mec-3(e1338)* were obtained from the Caenorhabditiis Genetics Center. Strain TV9696 *dma-1(wy686∷ ∷unc-119+)I*, was generated using the *Mos*Del [31] approach starting with strain IE22994.

Constructs and transgenes

Fosmids containing *C. elegans* genomic sequence (Geneservice) were manipulated using a previously described fosmid recombineering approach [28]. All other plasmid constructs were generated using yeast homologous recombination in a pRS413 backbone [44]. The *ser2prom3* (PVD), *Pmec-3* (FLP, PLM), *Pdat-1* (PDE) promoters were used for cell-specific expression. The following transgenic extrachromosomal arrays were generated via injection using standard techniques [45]: *wyEx3282(Pdma-1∷ ∷dma-1∷ ∷GFP∷ ∷SL2∷ ∷mcherry (fosmid))*, *wyEx3355(ser2prom3∷ ∷myrGFP)*, *wyEx4004(ser2prom3∷ ∷dma-1#1)*, *wyEx4005(ser2prom3∷ ∷dma-1#2)*, *wyEx4280(Pmec-3∷ ∷myrGFP)*, *wyEx4290(Pmec-3∷ ∷ dma-1)*, *wyEx4288(Pdma-1∷ ∷dma-1(fosmid))*, *wyEx3974(Pdat-1∷ ∷GFP)*, *wyEx4281(Pdat-1∷ ∷dma-1)*, *wyEx4289(Pmec-3∷ ∷dma-1)*, *wyEx4286(ser2prom3∷ ∷dma-1∷ ∷GFP). Podr-1∷ ∷RFP* (20ng/μl), *Pmyo-2∷ ∷mcherry* (2ng/μl), *Punc-122∷ ∷RFP* (20ng/μl), and *Ppha-1∷ ∷pha-1* (50ng/μl) were used as co-injection markers. Additional transgenic lines containing tagged extracellular LRR proteins are listed in Supplementary Table 1.

Fluorescence microscopy and confocal imaging

Images of fluorescent proteins were captured in live *C. elegans* using a Plan-Apochromat 63×/1.4 objective on a Zeiss LSM710 confocal microscope. Worms were immobilized using 10mM levamisole (Sigma). Z-stacks were collected and the maximum projection was used for additional analysis.

Quantification of branching

To measure the frequency of 2° and 2°′ branches, we always used the 1° dendritic process anterior of the PVD cell body for analysis. A 2° branch was defined as any distinguishable protrusion that extended away from the 1° process. The frequency of 2° branching was then calculated as the number of 2° branches per 100μm of the 1° dendritic process. 2°′ branches were defined as any branch that resulted from a branching event off a 2° process before reaching the 3° level. Again, frequency was measured per 100μm of the 1° dendritic process. To calculate the 3° branch Avoidance Index (AI), we counted the number of mature 2° branches (2° branches that extend 3° branches) and the number of distinct gaps between 3° branches. The AI is the ratio of gaps to mature 2° branches. All lengths were measured using ImageJ software.

RNA interference

Feeding RNAi was performed as previously described using the enhanced RNAi strain *rrf3(pk14246)II* and constructs from the Ahringer Lab library [46].

Harsh touch response

The assay to measure the response to harsh touch was performed as previously described [32]. A positive response was scored as movements of at least one body length in response to stimulus, though the speed of these movements can be variable in different mutant backgrounds.

Statistical analysis

Student's t-test and chi-square analysis were used to compare populations as indicated in the figure legends.

Supplementary Material

Refer to Web version on PubMed Central for supplementary material.

Acknowledgments

References

1. Masland RH. Neuronal cell types. Curr Biol. 2004; 14:R497–500. [PubMed: 15242626]

2. S, Ramon y Cajal. Histology of the Nervous System of Man and Vertebrates. Oxford University Press; 1995.

3. Wen Q, Stepanyants A, Elston GN, Grosberg AY, Chklovskii DB. Maximization of the connectivity repertoire as a statistical principle governing the shapes of dendritic arbors. Proc Natl Acad Sci U S A. 2009; 106:12536–41. [PubMed: 19622738]

4. Aizawa H, et al. Dendrite development regulated by CREST, a calcium-regulated transcriptional activator. Science. 2004; 303:197–202. [PubMed: 14716005]

5. Gaudilliere B, Konishi Y, de la Iglesia N, Yao G, Bonni A. A CaMKII-NeuroD signaling pathway specifies dendritic morphogenesis. Neuron. 2004; 41:229–41. [PubMed: 14741104]

6. Morita A, et al. Regulation of dendritic branching and spine maturation by semaphorin3A-Fyn signaling. J Neurosci. 2006; 26:2971–80. [PubMed: 16540575]

7. Grueber WB, et al. Projections of Drosophila multidendritic neurons in the central nervous system: links with peripheral dendrite morphology. Development. 2007; 134:55–64. [PubMed: 17164414]

8. Jan YN, Jan LY. Branching out: mechanisms of dendritic arborization. Nat Rev Neurosci. 2010; 11:316–28. [PubMed: 20404840]

9. Grueber WB, Jan LY, Jan YN. Different levels of the homeodomain protein cut regulate distinct dendrite branching patterns of Drosophila multidendritic neurons. Cell. 2003; 112:805–18. [PubMed: 12654247]

10. Sugimura K, Satoh D, Estes P, Crews S, Uemura T. Development of morphological diversity of dendrites in Drosophila by the BTB-zinc finger protein abrupt. Neuron. 2004; 43:809–22. [PubMed: 15363392]

11. Satoh D, et al. Spatial control of branching within dendritic arbors by dynein-dependent transport of Rab5-endosomes. Nat Cell Biol. 2008; 10:1164–71. [PubMed: 18758452]

12. Zheng Y, et al. Dynein is required for polarized dendritic transport and uniform microtubule orientation in axons. Nat Cell Biol. 2008; 10:1172–80. [PubMed: 18758451]

13. Sweeney NT, Brenman JE, Jan YN, Gao FB. The coiled-coil protein shrub controls neuronal morphogenesis in Drosophila. Curr Biol. 2006; 16:1006–11. [PubMed: 16713958]

14. Ye B, et al. Growing dendrites and axons differ in their reliance on the secretory pathway. Cell. 2007; 130:717–29. [PubMed: 17719548]

15. Jaworski J, Spangler S, Seeburg DP, Hoogenraad CC, Sheng M. Control of dendritic arborization by the phosphoinositide-3′-kinase-Akt-mammalian target of rapamycin pathway. J Neurosci. 2005; 25:11300–12. [PubMed: 16339025]

16. Emoto K, et al. Control of dendritic branching and tiling by the Tricornered-kinase/Furry signaling pathway in Drosophila sensory neurons. Cell. 2004; 119:245–56. [PubMed: 15479641]

17. Ye B, et al. Nanos and Pumilio are essential for dendrite morphogenesis in Drosophila peripheral neurons. Curr Biol. 2004; 14:314–21. [PubMed: 14972682]

18. Albeg A, et al. C. elegans multi-dendritic sensory neurons: Morphology and function. Mol Cell Neurosci. 2010

19. Smith CJ, et al. Time-lapse imaging and cell-specific expression profiling reveal dynamic branching and molecular determinants of a multi-dendritic nociceptor in C. elegans. Dev Biol. 2010; 345:18–33. [PubMed: 20537990]

20. Shen K, Cowan CW. Guidance molecules in synapse formation and plasticity. Cold Spring Harb Perspect Biol. 2010; 2:a001842. [PubMed: 20452946]

21. Shapiro L, Love J, Colman DR. Adhesion molecules in the nervous system: structural insights into function and diversity. Annu Rev Neurosci. 2007; 30:451–74. [PubMed: 17600523]

22. Dolan J, et al. The extracellular leucine-rich repeat superfamily; a comparative survey and analysis of evolutionary relationships and expression patterns. BMC Genomics. 2007; 8:320. [PubMed: 17868438]

23. Chen Y, Aulia S, Li L, Tang BL. AMIGO and friends: an emerging family of brain-enriched, neuronal growth modulating, type I transmembrane proteins with leucine-rich repeats (LRR) and cell adhesion molecule motifs. Brain Res Rev. 2006; 51:265–74. [PubMed: 16414120]

24. de Wit J, et al. LRRTM2 interacts with Neurexin1 and regulates excitatory synapse formation. Neuron. 2009; 64:799–806. [PubMed: 20064388]

25. Hong W, et al. Leucine-rich repeat transmembrane proteins instruct discrete dendrite targeting in an olfactory map. Nat Neurosci. 2009; 12:1542–50. [PubMed: 19915565]

26. Ko J, Fuccillo MV, Malenka RC, Sudhof TC. LRRTM2 functions as a neurexin ligand in promoting excitatory synapse formation. Neuron. 2009; 64:791–8. [PubMed: 20064387]

27. Linhoff MW, et al. An unbiased expression screen for synaptogenic proteins identifies the LRRTM protein family as synaptic organizers. Neuron. 2009; 61:734–49. [PubMed: 19285470]

28. Tursun B, Cochella L, Carrera I, Hobert O. A toolkit and robust pipeline for the generation of fosmid-based reporter genes in C. elegans. PLoS One. 2009; 4:e4625. [PubMed: 19259264]

29. Oren-Suissa M, Hall DH, Treinin M, Shemer G, Podbilewicz B. The fusogen EFF-1 controls sculpting of mechanosensory dendrites. Science. 2010; 328:1285–8. [PubMed: 20448153]

30. Tsalik EL, et al. LIM homeobox gene-dependent expression of biogenic amine receptors in restricted regions of the C. elegans nervous system. Dev Biol. 2003; 263:81–102. [PubMed: 14568548]

31. Frokjaer-Jensen C, et al. Targeted gene deletions in C. elegans using transposon excision. Nat Methods. 2010; 7:451–3. [PubMed: 20418868]

32. Way JC, Chalfie M. The mec-3 gene of Caenorhabditis elegans requires its own product for maintained expression and is expressed in three neuronal cell types. Genes Dev. 1989; 3:1823–33. [PubMed: 2576011]

33. Li W, Kang L, Piggott BJ, Feng Z, Xu XZ. The neural circuits and sensory channels mediating harsh touch sensation in Caenorhabditis elegans. Nat Commun. 2011; 2:315. [PubMed: 21587232]

34. Hutter H, Ng MP, Chen N. GExplore: a web server for integrated queries of protein domains, gene expression and mutant phenotypes. BMC Genomics. 2009; 10:529. [PubMed: 19917126]

35. Hattori D, Millard SS, Wojtowicz WM, Zipursky SL. Dscam-mediated cell recognition regulates neural circuit formation. Annu Rev Cell Dev Biol. 2008; 24:597–620. [PubMed: 18837673]

36. Dimitrova S, Reissaus A, Tavosanis G. Slit and Robo regulate dendrite branching and elongation of space-filling neurons in Drosophila. Dev Biol. 2008; 324:18–30. [PubMed: 18817767]

37. McAllister AK, Katz LC, Lo DC. Opposing roles for endogenous BDNF and NT-3 in regulating cortical dendritic growth. Neuron. 1997; 18:767–78. [PubMed: 9182801]

38. Long H, Ou Y, Rao Y, van Meyel DJ. Dendrite branching and self-avoidance are controlled by Turtle, a conserved IgSF protein in Drosophila. Development. 2009; 136:3475–84. [PubMed: 19783736]

39. Bella J, Hindle KL, McEwan PA, Lovell SC. The leucine-rich repeat structure. Cell Mol Life Sci. 2008; 65:2307–33. [PubMed: 18408889]

40. Morlot C, et al. Structural insights into the Slit-Robo complex. Proc Natl Acad Sci U S A. 2007; 104:14923–8. [PubMed: 17848514]

41. Schubert WD, et al. Structure of internalin, a major invasion protein of Listeria monocytogenes, in complex with its human receptor E-cadherin. Cell. 2002; 111:825–36. [PubMed: 12526809]

42. Caldwell JC, Fineberg SK, Eberl DF. reduced ocelli encodes the leucine rich repeat protein Pray For Elves in Drosophila melanogaster. Fly (Austin). 2007; 1:146–52. [PubMed: 18820435]

43. Aguirre-Chen C, Bulow HE, Kaprielian Z. C. elegans bicd-1, homolog of the Drosophila dynein accessory factor Bicaudal D, regulates the branching of PVD sensory neuron dendrites. Development. 2011; 138:507–18. [PubMed: 21205795]

44. Oldenburg KR, Vo KT, Michaelis S, Paddon C. Recombination-mediated PCR-directed plasmid construction in vivo in yeast. Nucleic Acids Res. 1997; 25:451–2. [PubMed: 9016579]

45. Mello C, Fire A. DNA transformation. Methods Cell Biol. 1995; 48:451–82. [PubMed: 8531738]

46. Wang GJ, et al. GRLD-1 regulates cell-wide abundance of glutamate receptor through post-transcriptional regulation. Nat Neurosci. 2010
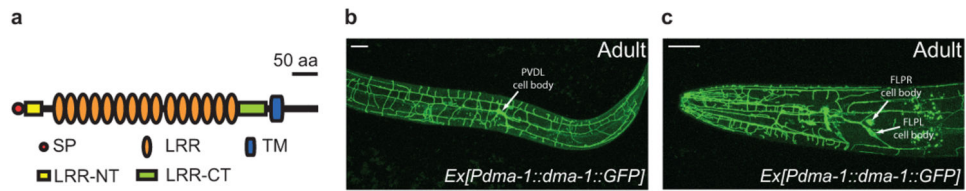
Figure 1.
DMA-1 is expressed in highly branched neurons

a, Schematic of DMA-1 protein structure including signal peptide (SP), leucine rich repeat N-terminal domain (LRR-NT), leucine-rich repeats (LRR), leucine rich repeat C-terminal domain (LRR-CT), and transmembrane (TM). **b-c**, Confocal images of adult worms expressing DMA-1 : :GFP under the control of its endogenous promoter. Strong expression is seen in the highly branched PVD and FLP neurons. Background autofluorescence is due to gut granules. Scale bars equal 20μm.
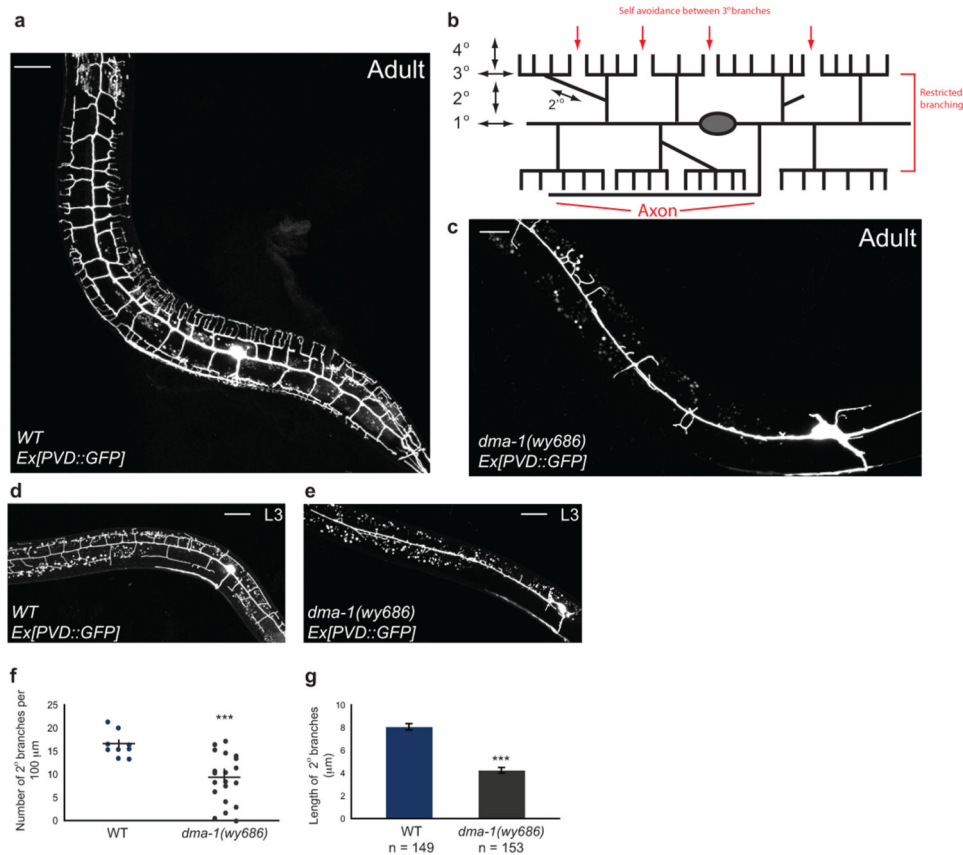
Figure 2. *dma-1* positively regulates PVD branching
a, PVD dendrites envelop the entire worm body. PVD can be labeled in its entirety with a cell specific marker (*PVD∷GFP*). **b**, Schematic of a stereotypical PVD neuron. PVD extends primary (1°) dendritic processes anteriorly and posteriorly from the cell body and a ventrally directed axonal process. Orthogonal branching (2°, 3°, 4°) generates a well-ordered array of candelabra-shaped arbors that demonstrates regulated branching and self-avoidance. **c**, Deletion of *dma-1* (the *dma-1(wy686)* allele) results in a fully-penetrant dendrite morphology defect in PVD. **d**, By the L3 larval stage, PVD has established 2° and 3° branching. **e**, *dma-1(wy686)* mutant L3 worms display easily quantifiable branching and growth defects. **f,** The density of 2° branching was determined by counting the number of 2° branches per 100 um of the anterior 1° process for a given worm. The distribution of densities was then compared for a wildtype and mutant population of worms. *dma-1(wy686)* mutant worms demonstrated a broad range of defects in 2° branch density with an average decrease of 44%. **g**, The average length of 2° branches decreased 47% compared to wild-type. All error bars shown represent s.e.m. *** $p < 0.0001$, t-test. Scale bars equal 20μm.
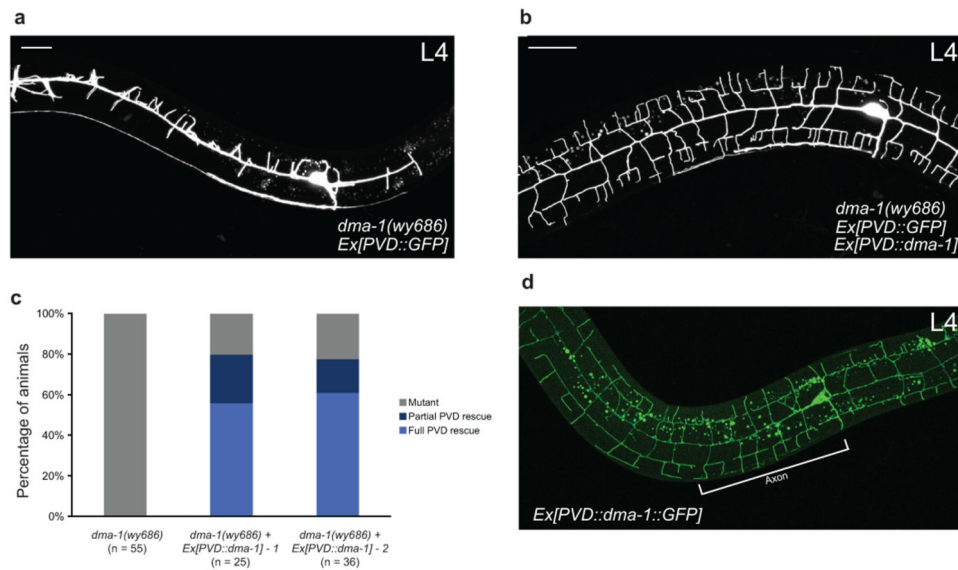
Figure 3.
DMA-1 functions cell autonomously
a-b, The dendrite morphology defect in *dma-1(wy686)* mutant animals can be cell-autonomously rescued by PVD-specific expression of *dma-1*. **c,** Quantification of cell-autonomous rescue of branching defects by cell-specific expression of *dma-1*. Two *dma-1(wy686)* lines carrying arrays expressing *PVD::dma-1* were generated. Worms carrying the array were categorized based on PVD morphology as mutant, partial PVD rescue, or full PVD rescue. Partial PVD rescue displayed some candelabra formation. Full PVD rescue was indistinguishable from wildtype PVD. **d**, Subcellular localization of GFP-tagged DMA-1 in PVD. DMA-1::GFP is found in all dendrite processes, but not in the axon. Scale bars equal 20μm.
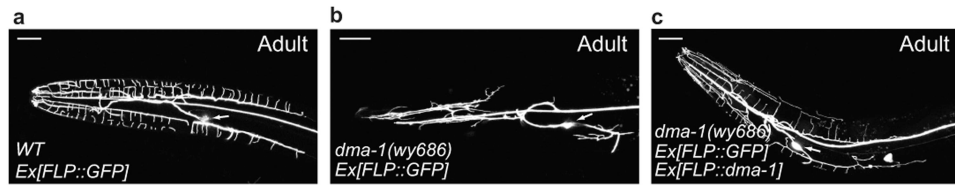
Figure 4. *dma-1* also regulates FLP branching

a, FLP neurons in the head elaborate highly branched dendrites similar to PVD. **b,** Deletion of *dma-1* results in a fully-penetrant dendrite morphology defect in FLP as well. **c**, This defect can be cell-autonomously rescued by FLP-specific expression of *dma-1*. Scale bars equal 20μm.

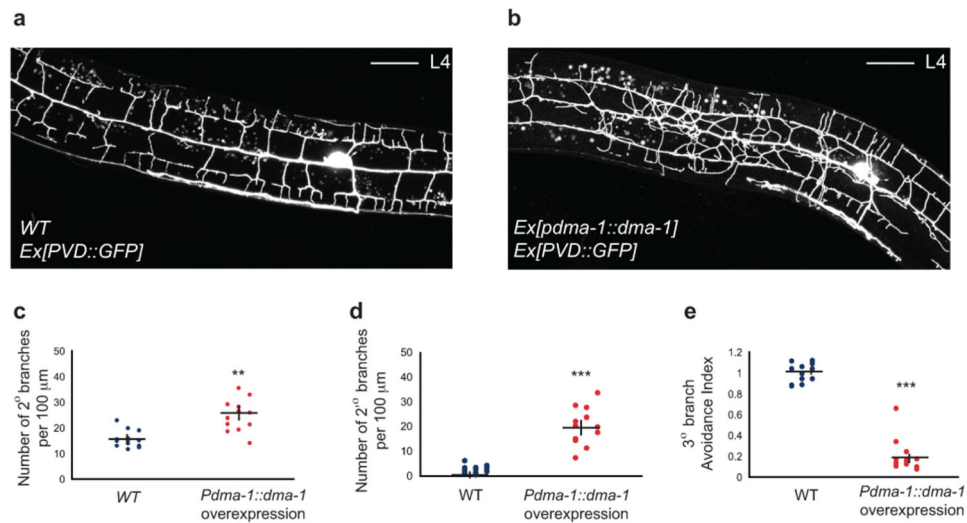**Figure 5. *dma-1* overexpression causes excessive branching**

a, By the L4 larval stage, PVD displays complete candelabra structures. **b,** Overexpression of *dma-1* results in excessive PVD branching. **c-d,** Quantification demonstrates significant increases in both 2° and 2°' branching. **b,e,** Overexpression of *dma-1* also results in a dramatic loss of sister dendrite self-avoidance between 3° level branches as measured by Avoidance Index. All error bars shown represent s.e.m. ** $p < 0.001$, *** $p < 0.0001$, t-test. Background autofluorescence is due to gut granules. Scale bars equal 20μm.
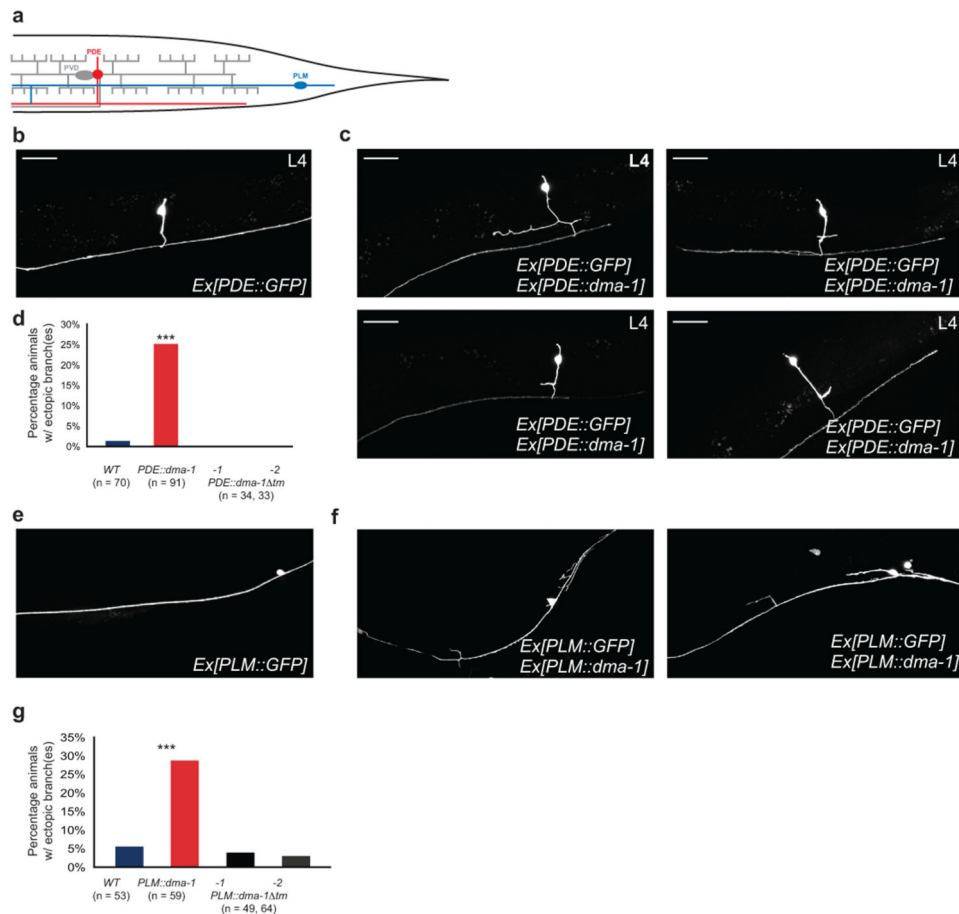
Figure 6. Expression of *dma-1* in morphologically simple neurons can induce ectopic branching
a, **b, e** PDE and PLM are morphologically simple sensory neurons with processes that run adjacent to PVD dendrites and can be labeled with cell-specific markers. **c**, Expression of *dma-1* in PDE causes orthogonal ectopic branching (arrows) at a stereotyped position in the PDE commissure, reminiscent in location and direction of PVD 3° branching. **d**, Ectopic branching at this stereotyped position is seen in 25% of animals carrying the *Ex[PDE::dma-1]* array, but not in animals carrying *Ex[PDE::dma-1 tm] arrays*. **f**, Expression of *dma-1* in PLM causes ectopic branching along the PLM process which runs laterally along the worm. **g**, Ectopic branching along PLM is seen in 29% of animals that carry the *Ex[PLM::dma-1]* array, but no increase in seen in animals carrying *Ex[PLM::dma-1 tm] arrays*. *** $p < 0.001$, chi-squared test. Scale bars equal 20μm.

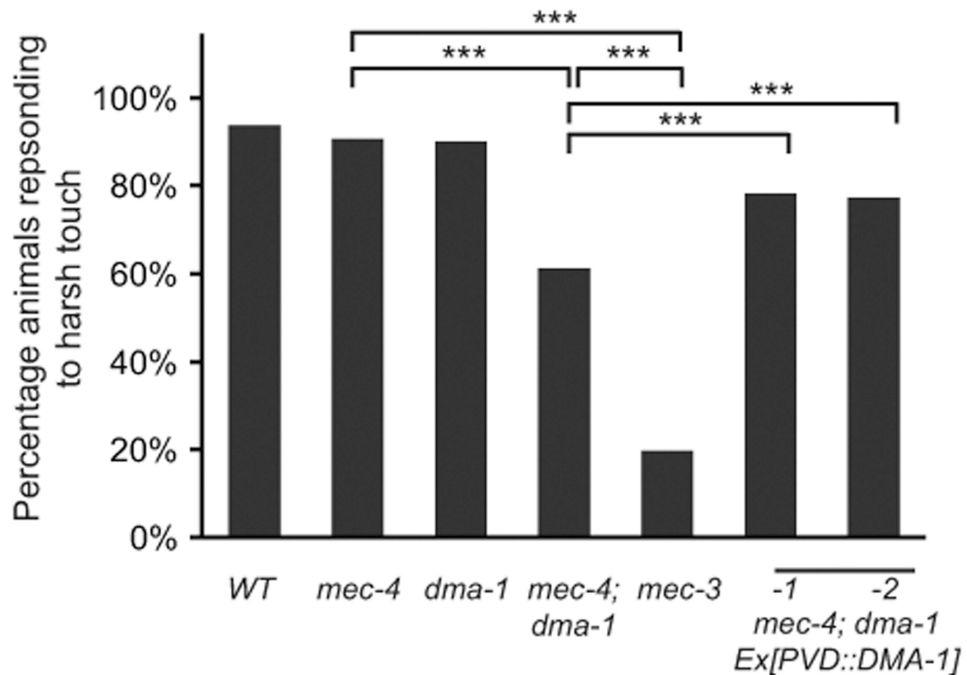

Figure 7. *dma-1* mutants display defects in response to harsh touch

Animals with the indicated genotypes were assayed for response to harsh touch. The *mec-4(u253)* mutation disables the touch receptor neurons (TRNs) allowing for the function of PVD in the harsh touch response to be isolated and assayed alone. As controls, *mec-4(u253)* and *dma-1(wy686)* single mutants responded similarly to WT. *mec-4(u253) dma-1(wy686)* double mutant animals demonstrated a significant defect in harsh touch response. As a control, the *mec-3(e1338)* mutation disables both the TRNs and PVD. Cell-specific expression of *dma-1* in PVD partially rescued the sensory defect detected in *mec-4(u253) dma-1(wy686)* double mutant animals. *** p < 0.001, chi-squared test